Adsorption of selected micropollutants on powdered activated carbon and biochar in the presence of kaolinite

Eunseon Kim[a], Chanil Jung[b], Jonghun Han[c], Namguk Her[c], Chang Min Park[d], Ahjeong Son[a,]*, Yeomin Yoon[d,]*

[a]*Department of Environmental Science and Engineering, Ewha Womans University, Seodaemun-gu, Seoul 120-750, Republic of Korea, Tel. +82 2 3277 3339; Fax: +82 2 3277 3275; email: ason@ewha.ac.kr (A. Son)*
[b]*Department of Earth and Environmental Studies, Montclair State University, Montclair, NJ 07043, USA*
[c]*Department of Civil and Environmental Engineering, Korea Army Academy at Young-Cheon, Kokyungmeon, Young-Cheon, Gyeongbuk 770-849, Republic of Korea*
[d]*Department of Civil and Environmental Engineering, University of South Carolina, Columbia, SC 29208, USA, Tel. +1 803 777 8952; Fax: +1 803 777 0670; email: yoony@cec.sc.edu (Y. Yoon)*

ABSTRACT

Commercially available powdered activated carbon (PAC) and activated biochar (produced in the laboratory), combined with kaolinite, were used to determine the adsorption of a beta-blocker (atenolol, ATN) and sunscreen compounds (benzophenone, BZP; and benzotriazole, BZT); a hypothesis was made that the presence of kaolinite would increase the adsorption of those target compounds. Various synthetic solutions were prepared by altering the pH, background ions, ionic strength, and glucose/humic acid content to mimic various natural water conditions. The removal efficiency of biochar–kaolinite was higher than that of PAC–kaolinite, presumably because the relatively high surface area and pore volume of biochar resulted in a higher adsorption capacity for the target compounds. Removal of the compounds in the absence of kaolinite followed the order BZP > ATN > BZT (*a* (mg/g); Langmuir maximum adsorption capacities were as follows: 85.0, 20.6, and 15.6 for PAC, and 125, 37.5, and 25.9 for biochar, respectively). An increase in the pH from 3.5 to 10.5 decreased the adsorption of ATN, BZP, and BZT by 14.5, 2.1, and 14.4%, respectively, by biochar–kaolinite. Additionally, an increase in background ions and their ionic strength, using NaCl, Na_2SO_4, and $CaCl_2$, increased the adsorption of the target compounds slightly, by 2.0–6.6%, depending on the target compound. Overall, biochar had a higher adsorption capacity for all chemicals tested compared with PAC, suggesting that biochar derived from loblolly pine chip may be a promising sorbent for water/wastewater treatment and environmental applications.

Keywords: Kaolinite; Micropollutants; Adsorption; Biochar; Nuclear magnetic resonance

*Corresponding authors.

1. Introduction

The presence of micropollutants, such as pharmaceuticals and personal care products (PPCPs), in drinking water and wastewater has emerged as a serious worldwide issue. Although PPCPs have been found at trace concentrations (<1 μg/L), some have been associated with ecological effects, even at low concentrations [1–6]. Due to the increasing use of sewage sludge for fertilizer and soil amendment in 2002, the US National Research Council recommended investigating the occurrence of PPCPs in sewage sludge [7]. Additionally, for other micropollutants, such as endocrine-disrupting compounds, the US Environmental Protection Agency announced the establishment of the Endocrine Disruptor Screening Program in 1998, which used a tiered approach to classify compounds with the potential to interfere with the endocrine system, to confirm that potential and characterize the effects of these chemicals [8].

Of the widely known PPCPs, atenolol (ATN), benzophenone (BZP), and benzotriazole (BZT) have been researched with respect to water and wastewater treatment [9–14]. ATN is a beta-blocker, affecting the heart and circulation, whereas BZP and BZT are widely used sunscreen agents. Conventional water and wastewater treatment processes, including coagulation, sedimentation, filtration, and secondary treatments, do not completely remove these micropollutants [2,15–17]. However, both "conventional" and emerging organic contaminants, such as pesticides, endocrine-disrupting compounds, and PPCPs, can be significantly removed using activated carbon adsorption [18,19]. The degree of removal by activated carbon adsorption is influenced significantly by the properties of both adsorbent (surface charge, surface area, pore size distribution, and oxygen content) and solute (hydrophobicity, size, charge, and shape) [20]. Hydrophobic interactions are the major removal mechanisms for most organic compounds in activated carbon adsorption systems, because activated carbon significantly removes most nonpolar organic compounds due to hydrophobic attraction [4].

Biochar, the by-product of the pyrolytic processing of biomass, has shown high potential as a promising adsorbent for micropollutant removal due to its highly condensed structure and surface density of functional groups [21,22]. These exceptional properties are controlled by activation, type of feedstock, and pyrolysis conditions (oxygen and hydrogen ratio, residence time, and temperature). Biochar pyrolyzed at a high temperature consists primarily of polyaromatic carbons and has a greater microporosity, which enhances organic compound adsorption, while greater proportions of aliphatic carbons and functional groups are typical of biochars pyrolyzed at lower temperatures [22,23]. Several recent studies have shown cost-effective adsorption with biochar to remove micropollutants, including sulfamethoxazole removal using a biochar pyrolyzed at 600°C [24], and sulfamethoxazole and sulfapyridine removal using demineralized pine wood biochar at 400 and 500°C [25].

Few studies have shown that inorganic and organic contaminants are removed by clays having various surface and structural properties, such as strong cation exchange capacity, low point of zero charge, large specific surface area, and high chemical/mechanical stability [26,27]. The sorption of triclosan and ibuprofen on kaolinite and montmorillonite was studied as a function of pH, ionic strength, and humic acid concentration [28,29]. However, there has been little research on the effects of minerals on biochar adsorption to remove micropollutants in aqueous solutions.
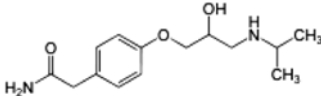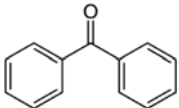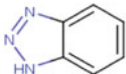
Thus, the objective of this study was to determine the effects of kaolinite on the removal of three target micropollutants (ATN, BZP, and BZT) having different physicochemical properties by biochar under various water quality conditions (pH, background ions, ionic strength, and natural organic matter (NOM, as described by glucose and humic acid)). Commercially available powdered activated carbon (PAC) was also examined for comparison. Activated biochar produced in the laboratory was characterized using advanced solid-state nuclear magnetic resonance (NMR) techniques as well as conventional analytical methods to address how these properties influence micropollutant adsorption.

2. Materials and methods

2.1. Materials

High purity (>99%) target PPCPs, glucose, and humic acid were obtained from Sigma-Aldrich (St. Louis, MO, USA). Table 1 shows the physicochemical properties of ATN, BZP, and BZT that were studied by spiking the compounds into various synthetic waters. In selecting the target compounds, two issues were considered: (i) their occurrence in drinking source waters and (ii) the physicochemical properties of the particular compound (e.g. hydrophobicity, size, and pK_a). The three compounds were dissolved together in methanol to produce high stock solutions (approximately 1,000 mg/L) to minimize the volume of solvents introduced into the experiments. Humic acid stock solution was prepared by adding 1 g of dry humic acid powder to 1 L of ultrapure deionized (DI)

Table 1
Properties of target micropollutants used in this study

Compound [ID] (use)	Structure	MW (g/mol)	Log D_{ow} [a]			Log K_{ow}	pK_a [a]
			pH 3.5	pH 7.0	pH 10.5		
Atenolol [ATN] (β-blocker)		266.3	0.43	0.43	−0.52	0.43	9.6
Benzophenone [BZP] (Sunscreen)		182.2	3.43	3.43	3.43	3.43	−7.5
Benzotriazole [BZT] (Sunscreen)		119.1	1.30	1.27	−1.01	1.30	8.2

[a]Chemicalize.org by ChemAxon (http://www.chemicalize.org).

water and stirring overnight. The solution was then filtered through 0.7-μm glass microfiber filters (Whatman, Buckinghamshire, UK) to remove particulate matter greater than 0.7 μm.

Biochar samples were produced in a laboratory-scale batch tube furnace (OTF-1200X, MTI Corp., Richmond, CA, USA) with torrefied loblolly pine chips (15 × 6 mm) at 300°C for 15 min under pure nitrogen. Loblolly pine chips containing bark were obtained from a local wood product industry and were torrefied using a pilot-scale torrefaction unit (about 1 ton/d capacity). A detailed description of the production method was published previously [30]. Briefly, biochar samples of 3 g were soaked in 40 mL of a 4 M NaOH solution and incubated with shaking (15-min interval) for 2 h at room temperature. The NaOH-impregnated biochar samples were then heated at 800°C for 2 h under a nitrogen gas flow (2 L/min) and cooled (10°C/min). Additionally, a commercially available powdered activated carbon (PAC, PAC form of F400, Calgon Carbon Corp., Pittsburgh, PA, USA) was used to compare its adsorption ability with that of the biochar prepared in the laboratory. Kaolinite in the form of kaolin was obtained from Junsei Chemical Co., Japan.

2.2. Adsorption experiments

The three selected micropollutants (ATN, BZP, and BZT) were studied by spiking them together into different synthetic waters. Initial concentrations of approximately 1,000 μg/L were placed in contact with PAC, biochar, and/or kaolinite as mixed components in binary mixtures with salts (NaCl, Na$_2$SO$_4$, or CaCl$_2$) or glucose/humic acid at various pH and ionic strength conditions. The stock solution of 1,000 mg/L of each adsorbent prepared in DI water was used for the batch adsorption experiments. Both kinetic and adsorbent dose-response experiments were conducted with 1, 4, and 24-h contact time with the applied adsorbent doses of PAC, biochar, and kaolinite ranging from 0 to 30 mg/L. PAC and biochar adsorption experiments in the presence of kaolinite were conducted at an adsorbent dose of 20 mg/L with a 4-h contact time. Many full-scale water treatment plants (WTPs) that use PAC have contact times of 1–5 h and apply PAC dosages of 5–50 mg/L. Kinetic experiments confirmed that 4 h was adequate time for the solution to reach a pseudo-equilibrium state, although adsorption experiments are commonly conducted for 7 d to reach equilibrium. Duplicate experiments were conducted in most experiments. Prior to the experiments, the pH of each solution was adjusted using 1 M HCl or 1 M NaOH solution and buffered with 2 mM phosphate buffer solution. The samples containing ATN, BZP, and BZT were placed in screw-cap amber vials (40 mL) spiked with the adsorbents for the kinetic and isotherm experiments and then placed in a shaker (Wise Shake SHO-2D, Seoul, South Korea) using a separate container for each duplicate at 100 rpm. Control treatments contained target micropollutants in the absence of PAC, biochar, and kaolinite. A 0.7-μm glass fiber filter (25 mm GF/F, Whatman International Ltd, Maidstone, England) was used to remove adsorbents from the samples.

The adsorption data obtained in the experiments were fitted to two different isotherm models:

Freundlich model: $q_e = K_f\, C_e^{1/n}$

Langmuir model: $q_e = \frac{abC_e}{1+bC_e}$

where q_e is the solid-phase concentration (mg/g), K_f is the Freundlich affinity coefficient ((mg/g)/(mg/L)$^{(1/n)}$), C_e is the equilibrium solution phase concentration (mg/L), n is a dimensionless number related to surface heterogeneity, a is the maximum adsorption capacity (mg/g), and b is the Langmuir fitting parameter (L/mg).

2.3. Characterization of adsorbents and analytical methods

The C, H, and N contents of PAC and biochar were determined using a PerkinElmer 2400 Series II elemental analyzer (PerkinElmer, Waltham, MA, USA). Average data for elemental compositions measured in duplicate are reported. Ash content was determined by heating the samples at 750°C, and the oxygen content was calculated from the mass difference with carbon, hydrogen, and nitrogen contents. The surface area using N_2 (SA-N_2) was determined by the Brunauer–Emmett–Teller (BET) method with a Gemini VII 2390p surface area analyzer (Micromeritics, Norcross, GA, USA), and the total pore volume was determined from the adsorbed quantity of N_2 at $P/P_0 = 0.95$. Solid-state direct-polarization magic-angle-spinning (DP/MAS) ^{13}C NMR spectra were obtained using a Varian Inova 500 spectrometer (Palo Alto, CA, USA). The ^{13}C NMR spectra, combined with dipolar-recoupled NMR methods, were used for quantitative structural analyses of the PAC and biochar. Detailed running parameters and chemical shift assignments for the NMR experiments are reported elsewhere [31]. The adsorption surface charge was determined as a function of pH for PAC and biochar at a concentration of 50 mg/L by zeta potential measurements (Brookhaven ZetaPALS, Holtsville, NY, USA).

Concentrations of ATN, BZP, and BZT were quantified using high-performance liquid chromatography coupled with mass spectrometry (HPLC-MS/MS) on Agilent Technologies 6410 and 1200 Series instruments (Santa Clara, CA, USA). HPLC-MS/MS was equipped with an electrospray ionization (ESI) apparatus and a C18 reverse column (150 × 4.6 mm, 5 μm) (Agilent Technologies, Santa Clara, CA, USA)). Chromatographically separated samples for HPLC-MS/MS were analyzed under the following conditions: ESI negative ionization mode; drying gas flow, 10 mL/min; nebulizer pressure, 345 kPa; drying gas temperature, 350°C; fragmentor, 110 V; collision energy, 25 V; precursor ion, 183 m/z; and product ion, 145 m/z for ATN, 105 m/z for BZP, and 65 m/z for BZT. The

concentration of each compound in the samples was determined against an external calibration curve with five different concentrations (1, 10, 50, 100, and 500 μg/L) prepared in DI water. Calibration standards of 50 μM were run between approximately every 10 samples. The method detection limits for the target compounds were approximately 1.0 μg/L.

3. Results and discussion

3.1. Characterization of PAC and biochar

Because adsorption is influenced mainly by the physicochemical properties of the adsorbent, characterization of the adsorbent is important. The precursor biochar for the activated biochar was pyrolyzed in the absence of oxygen, allowing the material to be fully charred. The commercially available PAC and activated biochar were characterized using both elemental analyses and solid-state NMR. The elemental composition and ^{13}C NMR spectra of PAC and biochar differed significantly, as shown in Table 2 and Fig. S1(a), while the elemental compositions of PAC and biochar were consistent with the ^{13}C solid-state NMR results. The carbon content (59.3%) of PAC was lower than that of biochar (72.6%), while the oxygen content (20.2%) of PAC was also slightly lower than that of biochar (21.3%). The H/C ratios were 0.032 and 0.127 for PAC and biochar, respectively, indicating that PAC was slightly more carbonized than biochar. Additionally, the relatively low H/C ratios indicate that both PAC and biochar were greatly thermally altered from the unsaturated material after dehydration [32]. A stronger peak at 108–148 ppm, corresponding to aryl carbons, showed that PAC has a more aromatic character than biochar, based on the ^{13}C DP/MAS NMR spectra. Additionally, PAC had a slightly lower aliphatic carbon fraction: paraffinic or alkyl (0–45 ppm), methoxyl (45–63 ppm), carbohydrate (63–108 ppm), and carboxyl carbons (165–187 ppm). Quantitative analyses of the ^{13}C DP/MAS experiments showed that biochar had a less condensed aromatic structure with lower aromaticity, based on the smaller nonprotonated carbon fraction, which agreed well with the higher H/C ratio than that of PAC. These results indicate that biochar has lower hydrophobicity than PAC.

The porous structures (BET surface area and pore volume) of PAC and biochar were determined through N_2 adsorption experiments. Higher surface area (1,360 m^2/g) and pore volume (0.95 cm^3/g) values were obtained for the chemically activated biochar than the commercial PAC (972 m^2/g and 0.53 cm^3/g, respectively), as shown in Table 2. This biochar may

Table 2
Properties of PAC and biochar modified from [30]

Elemental composition, aromatic ratio, ash content, BET-N_2 surface area ($SA-N_2$), and cumulative pore volume

Samples	C (%)	H (%)	N (%)	O (%)	H/C	Polarity index N/C	Polarity index O/C	Ash (%)	$SA-N_2$ (m²/g)	Pore volume (cm³/g) Micropore	Pore volume (cm³/g) Macropore
PAC	59.3	0.16	0.31	20.2	0.032	0.004	0.255	20.1	972.3	0.216	0.314
Biochar	72.6	0.77	0.65	21.3	0.127	0.001	0.221	4.7	1,360	0.307	0.643

Quantitative spectral analysis for solid-state ^{13}C DP/MAS NMR (calculated based on 100% carbon in each biomass)

Samples	Aliphatic C (%) Alkyl 0–45 ppm	Methoxyl 45–63 ppm	Carbo-hydrate 63–108 ppm	Aromatic C (%) Aryl 108–148 ppm	O-aryl 148–165 ppm	Carbonyls (%) Carboxyl 165–187 ppm	Carbonyl 187–220 ppm	Aromatic C (%)	Aliphatic C (%)	Aromaticity (%)[a]	Polar C (%)[b]
PAC	2.78	3.70	21.4	53.5	9.67	5.55	3.43	63.2	27.9	69.4	43.8
Biochar	7.14	4.81	21.5	45.7	9.91	8.22	2.79	55.6	33.5	62.5	47.2

[a] Aromaticity = aromatic C (108–165 ppm)/[aliphatic C (0–108 ppm) + aromatic C (108–165 ppm)].
[b] Total polar carbon = (45–108 ppm) + (148–220 ppm).

be a promising sorbent from a renewable biomass due to its high surface area and pore volume, which can possibly compete with coal-based activated carbons such as PAC. The amount of ash (4.7%) in the activated biochar was significantly lower than the commercial PAC (20.1%), presumably due to their properties as a feedstock, following the order of livestock manure > corn or wheat stover > hard wood > soft wood [33]. The correlation between the $SA-N_2$ of PAC/biochar and their ash contents showed that the $SA-N_2$ decreased with increasing ash content. It was expected that the higher ash content of coal-based PAC contributed little to the attraction between adsorbent and hydrophobic organic compounds, excluding the interaction with some ash-preferring species, such as some dyes and metal ions [34,35]. The pH at the point of zero charge (pH_{pzc}) is an important parameter to describe the efficiency of the adsorption process. The adsorbent surface becomes negatively charged under conditions of $pH > pH_{pzc}$, thus attracting or repelling target compounds, depending on their anionic or cationic functional groups. As shown in Fig. S1(b), the pH_{pzc} was nearly 9 for both PAC and biochar, although the pH_{pzc} of PAC was somewhat lower than that of biochar.

3.2. Kinetic and adsorbent dose-response experiments

Fig. S2 shows the removal kinetics of ATN, BZP, and BZT after 1, 4, and 24 h of contact with PAC, biochar, and kaolinite. The adsorption of those target compounds differed greatly among adsorbents: removal varied depending on the target compound, dose, and contact time. For example, 10, 5, and 30 mg/L of biochar were required to achieve approximately 30% ATN, BZP, and BZT removal, respectively, from the model water with a contact time of 1 h, whereas significantly lower doses were required for contact times of 4 and 24 h. Considerably higher doses were required for PAC to reach the same degree of adsorption, and the removal of these compounds by kaolinite was very low (approximately <10% regardless of compound type, dose, and contact time). The removal of BZP was the highest. The higher adsorption of BZP relative to ATN and BZT may be explained by its higher log K_{ow} (octanol–water partitioning coefficient) values (log K_{ow} = 3.43, 0.43, and 1.30, respectively), suggesting that hydrophobic interactions of the PPCPs with PAC and biochar are the governing adsorption mechanisms. Several other adsorption studies using PAC and biochar have also shown this mechanism [17,19,30].

Linearized Freundlich and Langmuir isotherm models were used to fit the adsorption of target

PPCPs by PAC and biochar, as shown in Fig. 1. Langmuir and Freundlich isotherms have often been used to describe the adsorption of organic contaminants by various adsorbents [16,36–38]. Langmuir isotherms describe single-layer adsorption, where the chemical only interacts with the PAC or biochar surface throughout adsorption. However, Freundlich isotherms describe multilayer adsorption, where the chemical interacts primarily with the adsorbent surfaces and then the chemicals react with each other. Table 3 lists the fitting parameters of both isotherm models for the adsorbents used in this study. Based on the high correlation values (R^2), adsorption by these adsorbents could be explained using either isotherm model. The log K_f values for the Freundlich model and the a values for the Langmuir model varied significantly among the target compounds, indicating that the adsorption capacities of the adsorbents were generally affected by the physicochemical properties of the compounds and the adsorbents. A clear trend of adsorption onto both PAC and biochar was observed for the target compounds: the removal of compounds followed the order BZP > ATN > BZT (K_f, (mg/g)/(mg/L)$^{1/n}$: 78.5, 19,3, and 9.47 for PAC, and

148, 37.3, and 16.0 for biochar; a (mg/g): 85.0, 20,6, and 15.6 for PAC, and 125, 37.5, and 25.9 for biochar, respectively). In addition, these adsorption phenomena are related to the water quality conditions (e.g., pH, ionic strength/background ion, and glucose/humic acid). The influence of these factors, as well as kaolinite, on the adsorption of target compounds is discussed in the following sections.

According to the Giles isotherm, the adsorption data for ATN, BZP, and BZT are classified into the Langmuir (L) type in which the adsorbents are progressively saturated with high relative affinity at low concentration of target PPCPs. The L-type isotherm is the most common for the sorption of organic chemicals on heterogeneous mixtures of adsorbents which sorbs organics to a different extent. The adsorption isotherms of BZP and BZT reach stricter asymptotic plateau having a limited sorption capacity than that of ATN.

The pseudo-second-order kinetic rate equation was applied to the experimental data as:

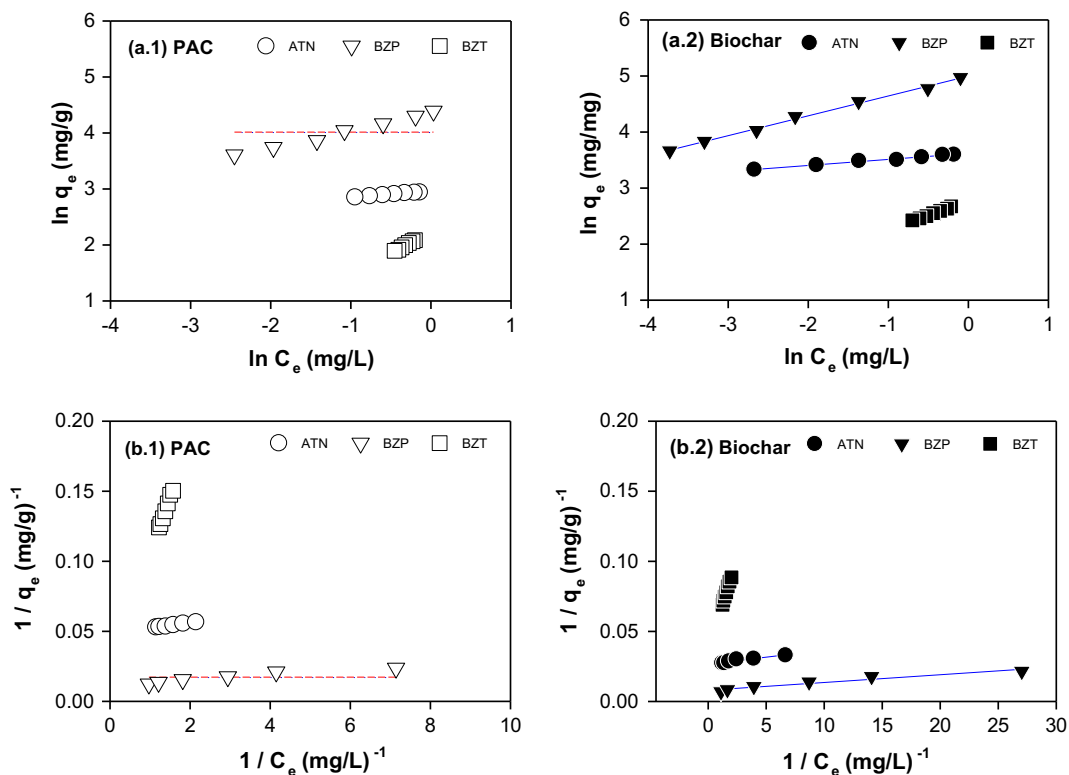$$\frac{dq_t}{dt} = k_2(q_e - q_t)^2$$

Fig. 1. (a) Freundlich and (b) Langmuir isotherms on the adsorption of ATN, BZP, and BZT onto PAC and biochar (contact time = 24 h; pH 7; NaCl = 10 mM).

Table 3
(a) Freundlich and (b) Langmuir isotherm parameters for adsorption of target micropollutants onto PAC and biochar (contact time = 24 h)

Adsorbate	PAC			Biochar		
	K_f ((mg/g)/(mg/L)$^{1/n}$)	$1/n$	R^2	K_f ((mg/g)/(mg/L)$^{1/n}$)	$1/n$	R^2
ATN	19.3	0.113	0.990	37.3	0.107	0.989
BZP	78.5	0.316	0.993	148	0.354	0.996
BZT	9.47	0.993	0.997	16.0	0.512	0.995
	a (mg/g)	b (L/mg)	R^2	a (mg/g)	b (L/mg)	R^2
ATN	20.6	12.7	0.990	37.5	27.0	0.930
BZP	85.0	6.46	0.940	125	14.5	0.936
BZT	15.6	0.36	0.992	25.9	1.53	0.991

where q_t is the concentration of PPCPs adsorbed on each adsorbent at time t (mg/g); and k_2 (g/mg/h) is the apparent diffusion rate constants. The values of k_2 and S_e are calculated from the slope and intercept of the linearized pseudo-second-order kinetic model plot. The adsorption kinetics well fitted to the pseudo-second-order kinetic model (Fig. S3, Table S1).

3.3. Effect of kaolinite

Kaolinite is a 1:1 dioctahedral clay mineral that has a two-layered structure consisting of a silicon–oxygen tetrahedral sheet linked to an alumina octahedral sheet. Use of naturally occurring kaolinite in the removal of different organic chemicals as a low-cost alternative adsorbent has been widely studied [28,29,39]. Because many full-scale WTPs that use PAC have contact times of 1–5 h and apply PAC dosages of 5–50 mg/L, PAC and biochar were combined with kaolinite in different ratios (20:0, 20:20, 20:50, and 20:100 mg/L) to examine the effects of kaolinite on the adsorption of the target PPCPs at a contact time of 4 h. Fig. 2 shows the adsorption of ATN, BZP, and BZT to adsorbents under all combination conditions. The original hypothesis was that the presence of kaolinite would increase the adsorption of target PPCPs. However, a trend of a slight decrease or similar sorption onto PAC or biochar combined with kaolinite from the 1:0 ratio to the 1:1 and 1:2 ratios was observed for the removal of these compounds. A potential mechanism can be proposed to account for the PPCP adsorption by PAC or biochar combined with kaolinite (approximately 2 μm [28]); physical pore blockage reduces the amount of surface area available for adsorption [40,41]. A slight increase in adsorption (approximately 5–15%) was obtained at a ratio of 1:5. This may be because the attractions (e.g., π–π electron donor–acceptor (EDA) and hydrophobic
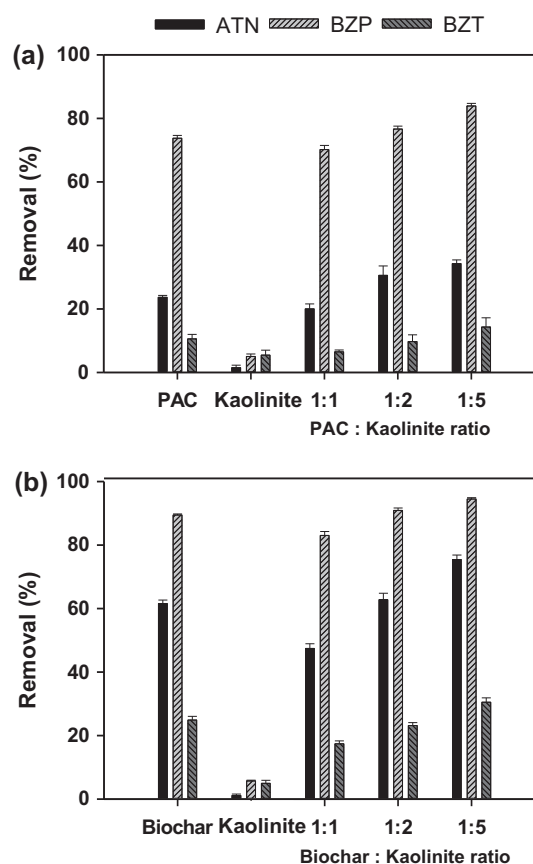

Fig. 2. Adsorption of target micropollutants on (a) PAC and (b) biochar in different PAC/biochar:kaolinite combinations (contact time = 4 h; each adsorbent dose = 20 mg/L; pH 7; NaCl = 10 mM).

interactions) between PPCPs and kaolinite contribute to their removal at the relatively high dosage condition [42]. A previous study showed very high adsorption (approximately 90%) of triclosan onto kaolinite (1,000 mg/L at pH 6) at a contact time of

24 h, suggesting that kaolinite can effectively remove micropollutants under optimal conditions [28]. However, to simulate a realistic range of adsorbents being used in WTPs, a 1:1 ratio of PAC or biochar to kaolinite was used for the remainder.

3.4. Effects of pH, adsorbates, and adsorbents

The effects of pH on the adsorption of ATN, BZP, and BZP are shown in Fig. 3. Target compounds that include single or multiple charged groups, as well as polar groups (hydroxyl and/or amine) with aromatic rings, are predominantly neutral species under acidic conditions, at pH 3.5 and 7. Generally, an increase in

the solution pH from 3.5 to 7 had a negligible effect (0.4–4.2%) on the adsorption of the compounds onto PAC–kaolinite and biochar–kaolinite. However, the adsorption decreased meaningfully, by 3–11.9%, with an increase in pH from 7 to 10.5. The difference between the decreases in the adsorption of the compounds under varying pH conditions may be attributable to the different log K_{ow} and pK_a values of each compound. The general decrease in adsorption may be the result of the increased ionization of the compounds caused by the increase in pH, possibly leading to reduced hydrophobic interactions with the adsorbents [43]. This is also presumably because electronic coupling influences the adsorptive interaction with each adsorbent. ATN, having a strong electron-withdrawing hydroxyl group, had a repulsive interaction with π—electron acceptor-rich aromatic rings on the adsorbents [21], resulting in inhibition of π–π EDA interactions. However, relatively less variation in adsorption affinity due to its negative pK_a and high log K_{ow} values caused BZP to show high adsorption (60.5–73.7% for PAC–kaolinite and 79.2–81.3% for biochar–kaolinite), presumably due to strong hydrophobic interactions over a wider range of pH values (Fig. 3). The adsorption difference based on log K_{ow} is true only if the compounds are nonionizable, independent of pH. Thus, use of the distribution coefficient (D) is more accurate and preferred, because it avoids the overestimation of hydrophobicity [44]. Table 1 summarizes the pH-dependent D values of the target compounds on a logarithmic scale at pH 3.5, 7.0, and 10.5. The adsorption of ATN and BZT decreased by 8.1–8.7% and 3.0–9.0%, respectively, with an increase in pH from 7.5 to 10.5, due to drops in hydrophobicity (log D_{ow} 0.43 to −0.52 for ATN and 1.27 to −1.01 for BZT), thus lowering the interaction with the adsorbent when pH > pK_a. The adsorption of ATN was meaningfully higher than that of BZT, although ATN had somewhat lower log D_{ow} values (0.43) at pH 3.5 and 7 than BZT (1.30–1.27). This is presumably because the adsorptive interactions of ATN with the adsorbents were still strongly related to π–π dispersion interactions between the adsorbate aromatic ring (electron acceptor) and the adsorbents [45].

The adsorption of all organic compounds cannot be described simply by one or two mechanisms, such as hydrophobic interactions, although many previous studies have emphasized those mechanisms in various solutions [17,19,30]. In this study, overall findings showed that biochar was more effective at removing all target compounds than PAC with and/or without kaolinite (Figs. 1–5), even though biochar has a lower aromaticity (62.5%) than PAC (69.4%). The larger surface area and pore volume of biochar relative to
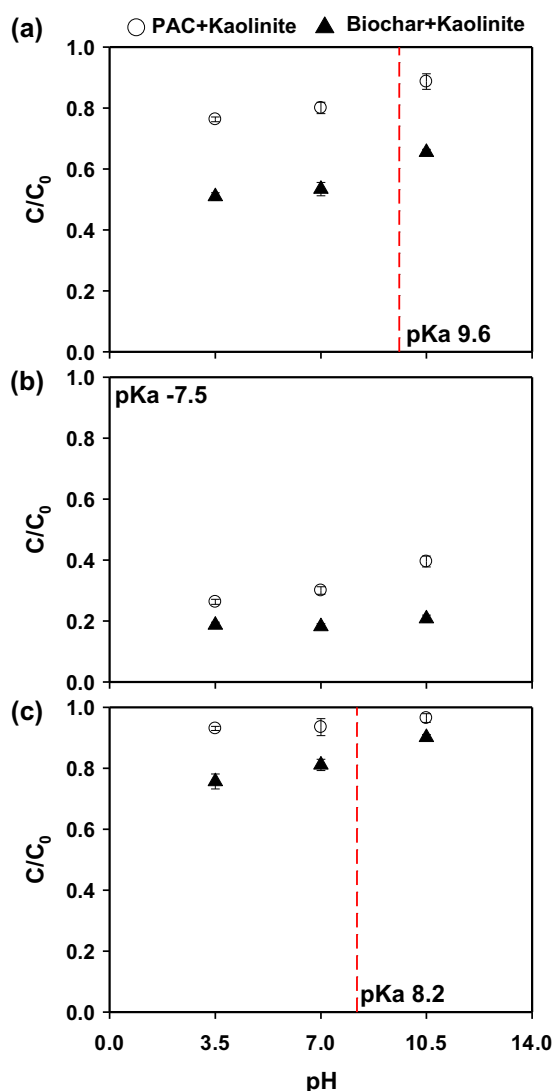
Fig. 3. Effect of pH on adsorption by PAC and biochar combined with kaolinite (contact time = 4 h; adsorbent dose = 20 mg/L:20 mg/L (PAC/biochar:kaolinite); NaCl = 10 mM). (a) ATN, (b) BZP, and (c) BZT.

PAC significantly enhanced its adsorption capacity (Table 2), while the high aromaticity contributed to effective adsorption [46]. Additionally, adsorption performance was influenced significantly by structural characteristics, surface properties, and the elemental composition of the adsorbents. Previous studies have shown that micropore filling and sieving effects meaningfully influenced the adsorption capacity of organic compounds [21,47,48]. Biochar had relatively smaller pore filling and sieving effects due to its larger micro- and macro-pore volumes (0.307 and 0.643 cm^3/g) compared with those of PAC (0.216 and 0.314 cm^3/g, respectively; Table 2). The adsorption behavior might also be attributable to π–H-bonding interactions due to

the greater portion of O-containing (polar) functional groups in biochar [49]. Larger contributions of carbohydrate (63–108 ppm), carboxyl (165–187 ppm), and carbonyl carbons (187–220 ppm), as obtained from the ^{13}C NMR spectra in biochar, are attributable to polar functional groups, indicating that a polarity provider induces a higher adsorption capacity. Additionally, the relatively high polarity of biochar, based on its polarity index (N/C + O/C), enhanced the adsorption attraction toward polar compounds due to delocalization of the aromatic π-cloud. This role of polarizability may cause induced electrostatic interactions (i.e. π–π interaction, π-stacking, and London dispersion forces [50]).
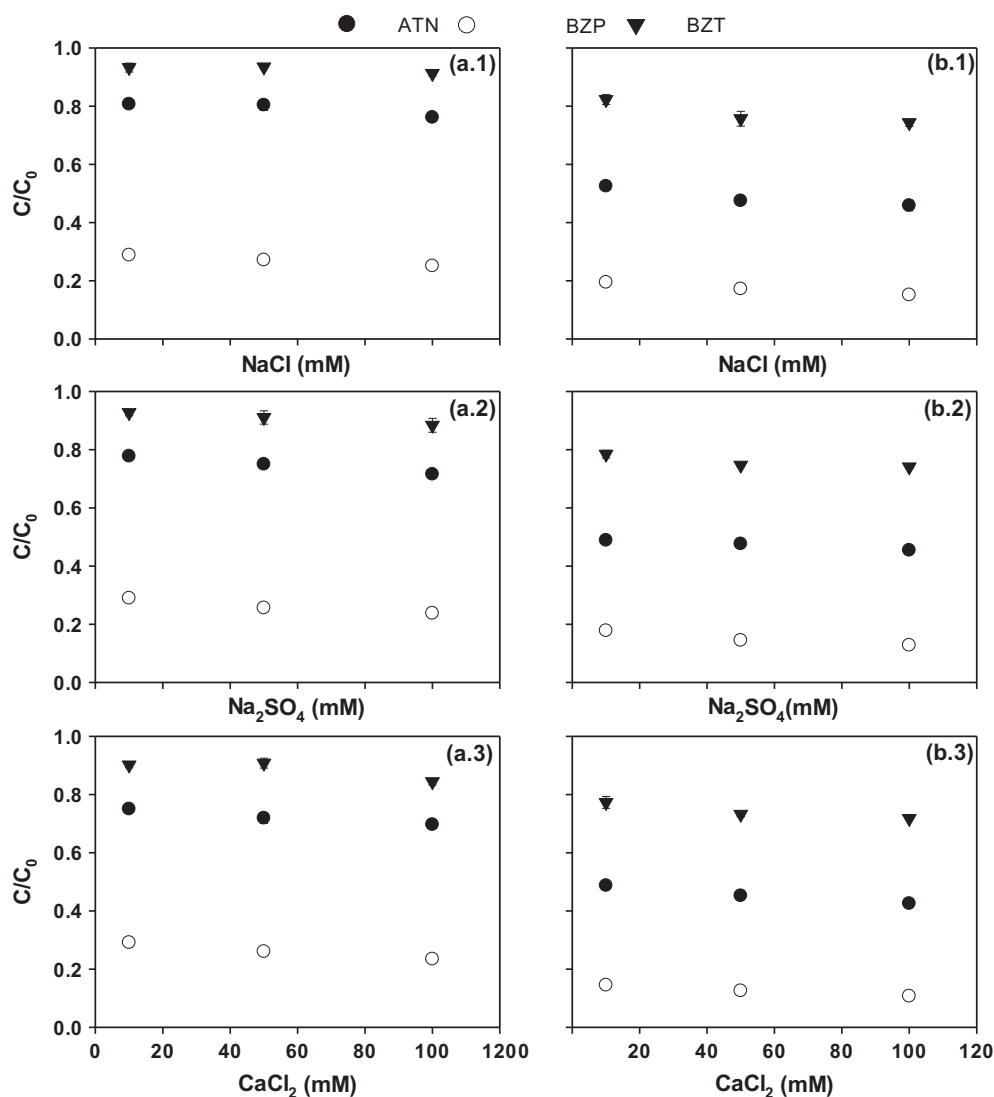

Fig. 4. Effect of background ions on adsorption by (a) PAC and (b) biochar combined with kaolinite (contact time = 4 h; adsorbent dose = 20 mg/L:20 mg/L (PAC/biochar:kaolinite); pH 7).

3.5. Effects of electrolyte species and ionic strength

The effects of electrolyte species on the adsorption of ATN, BZP, and BZT onto PAC–kaolinite and biochar–kaolinite were examined by varying the concentrations of NaCl, Na_2SO_4, and $CaCl_2$ (10, 50, and 100 mM). As shown in Fig. 4, generally, the adsorption of the compounds by both PAC–kaolinite and biochar–kaolinite increased slightly with increasing concentrations of background ions (2.0–6.6%). All background ions showed similar effects on adsorption for PAC–kaolinite and biochar–kaolinite, while the overall removal trend of compounds followed the order $CaCl_2$ > NaCl $\cong$ Na_2SO_4 in the presence of varying background ions. This finding can perhaps be understood by the previously mentioned "salting-out" effect (i.e. organic compound solubility decreases in aqueous salt solutions), which has been observed to be strong with Na^+ and Ca^{2+} [51]. This mechanism could increase the availability of the PAC–kaolinite and biochar–kaolinite surfaces to the target compounds. Several previous studies have revealed that the adsorption of compounds onto carbonaceous materials can be enhanced with increasing ionic strength due to a screening effect of the surface charge, produced by adding a salt [52,53]. Theoretically,

adsorbent particles and compound molecules are both enclosed by an electric double layer due to electrostatic interactions. Based on the Gouy–Chapman theory of the diffuse double layer, the thickness of the double layer is compressed by an increase in the ionic strength of the solution [54]. Thus, the adsorption of the target compounds can be enhanced at higher ionic strength due to the incomplete neutralization of the positive charge on the adsorbent surface and a resulting compression of the electrical double layer by the background ions [28].

3.6. Effects of glucose and humic acid

Competitive adsorption was evaluated in the presence of glucose (180 g/mol) and humic acid (approximately 600 g/mol used in this study), representing the relatively simple and complex organic carbon present in natural water, respectively. Fig. 5 shows the effects of glucose and humic acid on the adsorption of target compounds on PAC–kaolinite and biochar–kaolinite. An increase in the concentration of glucose did not significantly affect target compound adsorption (<3.1% increase with increasing glucose dose), presumably due to the hydrophilic nature of glucose. However, a
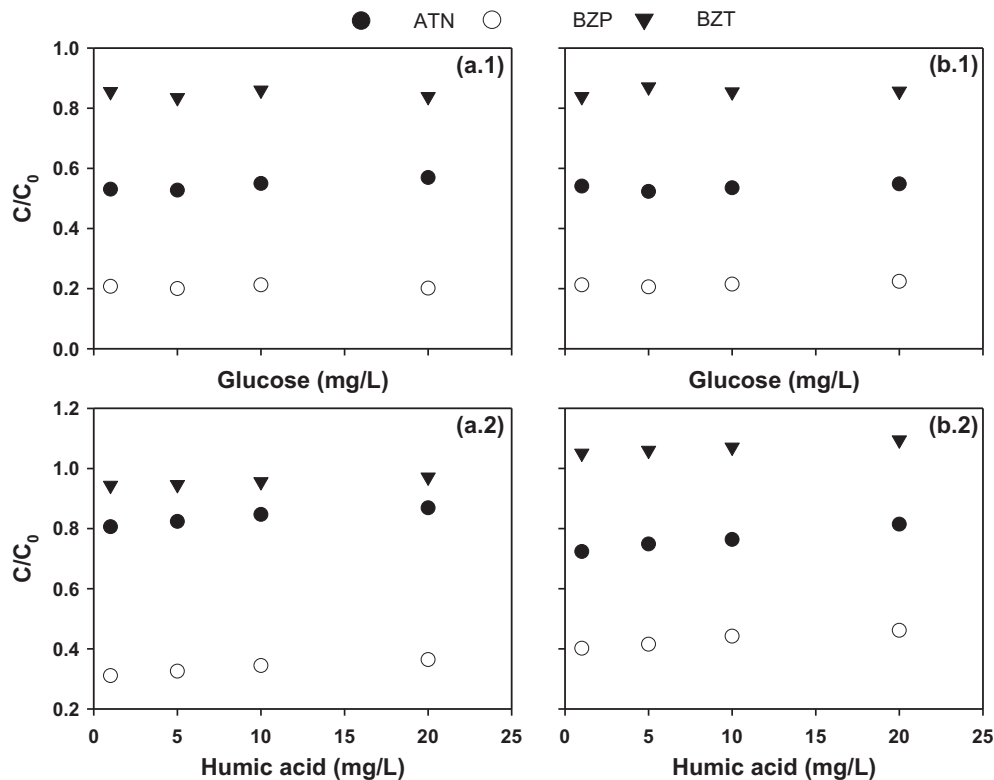

Fig. 5. Effect of glucose and humic acid on adsorption by PAC and biochar combined with kaolinite (contact time = 4 h; adsorbent dose = 20 mg/L:20 mg/L (PAC/biochar:kaolinite); pH 7; NaCl = 10 mM).

relatively higher decrease in the adsorption of the target compounds was observed with the addition of humic acid (by 3.1–6.4% for PAC–kaolinite and 4.9–8.9% for biochar–kaolinite), depending on each compound. Generally, a main mechanism (i.e. direct site competition) is believed to affect activated carbon adsorption in the presence of NOM. A previous study related to the effects of NOM on adsorption of micropollutants onto activated carbon showed that the mechanism for micropollutant adsorption competition is mainly the direct site competition [55,56].

4. Conclusions

Overall, the findings of this study demonstrate that biochar produced in the laboratory has higher removal efficiencies for the target PPCPs (ATN, BZP, and BZT) regardless of water quality conditions in the absence and presence of kaolinite compared with commercially available PAC. This is presumably because biochar has higher polarity moieties, with more alkyl, methoxyl, O-alkyl, and carboxyl carbon contents than PAC, as well as its larger surface area and pore volume. Unlike our original hypothesis that the presence of kaolinite would enhance the adsorption of target PPCPs, a trend of a slight increase, decrease, or similar sorption onto PAC or biochar combined with kaolinite was observed for the removal of these compounds, depending on the ratio of PAC or biochar to kaolinite. The adsorptive capacity of both adsorbents in the absence and presence of kaolinite consistently followed the order BZP > ATN > BZT, presumably due to differences in their physicochemical properties. An increase in pH decreased the adsorption somewhat, presumably due to electronic coupling affecting the adsorptive interaction with each adsorbent. Additionally, increases in ionic strength, when adjusted with NaCl, Na_2SO_4, and $CaCl_2$, resulted in a slight increase in adsorption, presumably due to "salting-out" and screening effects. In this study, glucose had a negligible effect on the adsorption onto the adsorbents, while humic acid slightly decreased the adsorption of the PPCPs. This observation can be explained either by direct competition between the PPCPs and humic acid for adsorption sites on the adsorbents or limited access to adsorbent surfaces due to pore blockage caused by the hydrophobic humic acid.

Supplementary material

The supplementary material for this paper is available online at http://dx.doi.[10.1080/19443994.2016. 1175972].

References

[1] M.J. Benotti, B.J. Brownawell, Distributions of pharmaceuticals in an urban estuary during both dry-and wet-weather conditions, Environ. Sci. Technol. 41 (2007) 5795–5802.

[2] J. Ryu, Y. Yoon, J. Oh, Occurrence of endocrine disrupting compounds and pharmaceuticals in 11 WWTPs in Seoul, Korea, KSCE J. Civ. Eng. 15 (2011) 57–64.

[3] S. Snyder, B. Vanderford, R. Pearson, O. Quiñones, Y. Yoon, Analytical methods used to measure endocrine disrupting compounds in water, Pract. Period. Hazard. Toxic Radioact. Waste Manage. 7 (2003) 224–234.

[4] S.A. Snyder, P. Westerhoff, Y. Yoon, D.L. Sedlak, Pharmaceuticals, personal care products, and endocrine disruptors in water: Implications for the water industry, Environ. Eng. Sci. 20 (2003) 449–469.

[5] T.A. Ternes, Occurrence of drugs in German sewage treatment plants and rivers, Water Res. 32 (1998) 3245–3260.

[6] Y. Yoon, J. Ryu, J. Oh, B.G. Choi, S.A. Snyder, Occurrence of endocrine disrupting compounds, pharmaceuticals, and personal care products in the Han River (Seoul, South Korea), Sci. Total Environ. 408 (2010) 636–643.

[7] NRC, Biosolids Applied to Land: Advancing Standards and Practices, 2002. Available from: <http://water.epa.gov/scitech/wastetech/biosolids/>.

[8] USEPA, Environmental Protection Agency—Endocrine Disruptor Screening Program, Report to Congress, USEPA, Washington, DC, 2000.

[9] J. Altmann, A.S. Ruhl, F. Zietzschmann, M. Jekel, Direct comparison of ozonation and adsorption onto powdered activated carbon for micropollutant removal in advanced wastewater treatment, Water Res. 55 (2014) 185–193.

[10] S.-H. Lee, C.-G. Park, Y. Onoda, N. Satou, A. Tabata, S.-H. Lee, B.-D. Lee, Characteristics of pharmaceuticals removal in the sewage treatment process, Desalin. Water Treat. 54 (2015) 1080–1089.

[11] J. Löwenberg, A. Zenker, M. Baggenstos, G. Koch, C. Kazner, T. Wintgens, Comparison of two PAC/UF processes for the removal of micropollutants from wastewater treatment plant effluent: Process performance and removal efficiency, Water Res. 56 (2014) 26–36.

[12] A.S. Ruhl, F. Zietzschmann, I. Hilbrandt, F. Meinel, J. Altmann, A. Sperlich, M. Jekel, Targeted testing of activated carbons for advanced wastewater treatment, Chem. Eng. J. 257 (2014) 184–190.

[13] J.L. Sotelo, A. Rodriguez, S. Alvarez, J. Garcia, Removal of caffeine and diclofenac on activated carbon in fixed bed column, Chem. Eng. Res. Des. 90 (2012) 967–974.

[14] L. Hernández-Leal, H. Temmink, G. Zeeman, C.J.N. Buisman, Removal of micropollutants from aerobically treated grey water via ozone and activated carbon, Water Res. 45 (2011) 2887–2896.

[15] M.J. Benotti, R.A. Trenholm, B.J. Vanderford, J.C. Holady, B.D. Stanford, S.A. Snyder, Pharmaceuticals and endocrine disrupting compounds in U.S. Drinking Water, Environ. Sci. Technol. 43 (2008) 597–603.

[16] L. Joseph, L.K. Boateng, J.R. Flora, Y.-G. Park, A. Son, M. Badawy, Y. Yoon, Removal of bisphenol A and 17α-ethinyl estradiol by combined coagulation and adsorption using carbon nanomaterials and powdered activated carbon, Sep. Purif. Technol. 107 (2013) 37–47.

[17] P. Westerhoff, Y. Yoon, S. Snyder, E. Wert, Fate of endocrine-disruptor, pharmaceutical, and personal care product chemicals during simulated drinking water treatment processes, Environ. Sci. Technol. 39 (2005) 6649–6663.

[18] S.A. Snyder, S. Adham, A.M. Redding, F.S. Cannon, J. DeCarolis, J. Oppenheimer, E.C. Wert, Y. Yoon, Role of membranes and activated carbon in the removal of endocrine disruptors and pharmaceuticals, Desalination 202 (2007) 156–181.

[19] Y.M. Yoon, P. Westerhoff, S.A. Snyder, M. Esparza, HPLC-fluorescence detection and adsorption of bisphenol A, 17β-estradiol, and 17α-ethynyl estradiol on powdered activated carbon, Water Res. 37 (2003) 3530–3537.

[20] C. Jung, L.K. Boateng, J.R. Flora, J. Oh, M.C. Braswell, A. Son, Y. Yoon, Competitive adsorption of selected non-steroidal anti-inflammatory drugs on activated biochars: Experimental and molecular modeling study, Chem. Eng. J. 264 (2015) 1–9.

[21] L. Ji, F. Liu, Z. Xu, S. Zheng, D. Zhu, Adsorption of pharmaceutical antibiotics on template-synthesized ordered micro- and mesoporous carbons, Environ. Sci. Technol. 44 (2010) 3116–3122.

[22] B. Chen, D. Zhou, L. Zhu, Transitional adsorption and partition of nonpolar and polar aromatic contaminants by biochars of pine needles with different pyrolytic temperatures, Environ. Sci. Technol. 42 (2008) 5137–5143.

[23] Y. Chun, G. Sheng, C.T. Chiou, B. Xing, Compositions and sorptive properties of crop residue-derived chars, Environ. Sci. Technol. 38 (2004) 4649–4655.

[24] T. Li, X. Han, C. Liang, M. Shohag, X. Yang, Sorption of sulphamethoxazole by the biochars derived from rice straw and alligator flag, Environ. Technol. 36 (2014) 1–9.

[25] M. Xie, W. Chen, Z. Xu, S. Zheng, D. Zhu, Adsorption of sulfonamides to demineralized pine wood biochars prepared under different thermochemical conditions, Environ. Pollut. 186 (2014) 187–194.

[26] B. Lombardi, R. Sanchez, P. Eloy, M. Genet, Interaction of thiabendazole and benzimidazole with montmorillonite, Appl. Clay Sci. 33 (2006) 59–65.

[27] G. Rytwo, D. Tropp, C. Serban, Adsorption of diquat, paraquat and methyl green on sepiolite: Experimental results and model calculations, Appl. Clay Sci. 20 (2002) 273–282.

[28] S. Behera, S. Oh, H. Park, Sorption of triclosan onto activated carbon, kaolinite and montmorillonite: Effects of pH, ionic strength, and humic acid, J. Hazard. Mater. 179 (2010) 684–691.

[29] S. Behera, S. Oh, H. Park, Sorptive removal of ibuprofen from water using selected soil minerals and activated carbon, Int. J. Environ. Sci. Technol. 9 (2012) 85–94.

[30] C. Jung, J. Park, K.H. Lim, S. Park, J. Heo, N. Her, J. Oh, S. Yun, Y. Yoon, Adsorption of selected endocrine disrupting compounds and pharmaceuticals on activated biochars, J. Hazard. Mater. 263 (2013) 702–710.

[31] J. Park, J. Meng, K.H. Lim, O.J. Rojas, S. Park, Transformation of lignocellulosic biomass during torrefaction, J. Anal. Appl. Pyrolysis 100 (2013) 199–206.

[32] M. Keiluweit, P.S. Nico, M.G. Johnson, M. Kleber, Dynamic molecular structure of plant biomass-derived black carbon (biochar), Environ. Sci. Technol. 44 (2010) 1247–1253.

[33] D.A. Laird, R.C. Brown, J.E. Amonette, J. Lehmann, Review of the pyrolysis platform for coproducing bio-oil and biochar, Biofuels, Bioprod. Biorefin. 3 (2009) 547–562.

[34] B. Hameed, A. Ahmad, N. Aziz, Isotherms, kinetics and thermodynamics of acid dye adsorption on activated palm ash, Chem. Eng. J. 133 (2007) 195–203.

[35] M. Ahmaruzzaman, Role of Fly Ash in the removal of organic pollutants from wastewater, Energy Fuels 23 (2009) 1494–1511.

[36] L. Joseph, J.R.V. Flora, Y.-G. Park, M. Badawy, H. Saleh, Y. Yoon, Removal of natural organic matter from potential drinking water sources by combined coagulation and adsorption using carbon nanomaterials, Sep. Purif. Technol. 95 (2012) 64–72.

[37] L. Joseph, J. Heo, Y.-G. Park, J.R.V. Flora, Y. Yoon, Adsorption of bisphenol A and 17α-ethinyl estradiol on single walled carbon nanotubes from seawater and brackish water, Desalination 281 (2011) 68–74.

[38] S.-W. Nam, D.-J. Choi, S.-K. Kim, N. Her, K.-D. Zoh, Adsorption characteristics of selected hydrophilic and hydrophobic micropollutants in water using activated carbon, J. Hazard. Mater. 270 (2014) 144–152.

[39] T.A. Khan, S. Dahiya, I. Ali, Use of kaolinite as adsorbent: Equilibrium, dynamics and thermodynamic studies on the adsorption of Rhodamine B from aqueous solution, Appl. Clay Sci. 69 (2012) 58–66.

[40] M. Arias, M.T. Barral, J.C. Mejuto, Enhancement of copper and cadmium adsorption on kaolin by the presence of humic acids, Chemosphere 48 (2002) 1081–1088.

[41] S.S. Tahir, N. Rauf, Removal of a cationic dye from aqueous solutions by adsorption onto bentonite clay, Chemosphere 63 (2006) 1842–1848.

[42] M. Kleber, P. Sollins, R. Sutton, A conceptual model of organo-mineral interactions in soils: Self-assembly of organic molecular fragments into zonal structures on mineral surfaces, Biogeochemistry 85 (2007) 9–24.

[43] K. Yang, W. Wu, Q. Jing, L. Zhu, Aqueous adsorption of aniline, phenol, and their substitutes by multi-walled carbon nanotubes, Environ. Sci. Technol. 42 (2008) 7931–7936.

[44] K. Kümmerer, Pharmaceuticals in the Environment: Sources, Fate, Effects and Risks, Springer Verlag, Berlin, 2004.

[45] L.F. Delgado, P. Charles, K. Glucina, C. Morlay, Adsorption of ibuprofen and atenolol at trace concentration on activated carbon, Sep. Sci. Technol. 50 (2015) 1487–1496.

[46] K. Sun, K. Ro, M. Guo, J. Novak, H. Mashayekhi, B. Xing, Sorption of bisphenol A, 17α-ethinyl estradiol and phenanthrene on thermally and hydrothermally produced biochars, Bioresour. Technol. 102 (2011) 5757–5763.

[47] D. Zhu, J.J. Pignatello, Characterization of aromatic compound sorptive interactions with black carbon (charcoal) assisted by graphite as a model, Environ. Sci. Technol. 39 (2005) 2033–2041.

[48] T.H. Nguyen, H.H. Cho, L. Dianne, W.P. Ball, Evidence for a pore-filling mechanism in the adsorption of aromatic hydrocarbons to a natural wood char, Environ. Sci. Technol. 41 (2007) 1212–1217.

[49] K. Sun, B. Gao, Z. Zhang, G. Zhang, Y. Zhao, B. Xing, Sorption of atrazine and phenanthrene by organic matter fractions in soil and sediment, Environ. Pollut. 158 (2010) 3520–3526.

[50] C.R. Martinez, B.L. Iverson, Rethinking the term "pi-stacking", Chem. Sci. 3 (2012) 2191–2201.

[51] M.A. Schlautman, S.B. Yim, E.R. Carraway, J.H. Lee, B.E. Herbert, Testing a surface tension-based model to predict the salting out of polycyclic aromatic hydrocarbons in model environmental solutions, Water Res. 38 (2004) 3331–3339.

[52] M.A. Fontecha-Cámara, M.V. López-Ramón, M.A. Álvarez-Merino, C. Moreno-Castilla, Effect of surface chemistry, solution pH, and ionic strength on the removal of herbicides diuron and amitrole from water by an activated carbon fiber, Langmuir 23 (2007) 1242–1247.

[53] A. Vinu, K.Z. Hossain, G.S. Kumar, K. Ariga, Adsorption of l-histidine over mesoporous carbon molecular sieves, Carbon 44 (2006) 530–536.

[54] M. Rashid, D. Buckley, K. Robertson, Interactions of a marine humic acid with clay minerals and a natural sediment, Geoderma 8 (1972) 11–27.

[55] Y. Matsui, Y. Fukuda, T. Inoue, T. Matsushita, Effect of natural organic matter on powdered activated carbon adsorption of trace contaminants: Characteristics and mechanism of competitive adsorption, Water Res. 37 (2003) 4413–4424.

[56] J. Hu, A. Martin, R. Shang, W. Siegers, E. Cornelissen, B. Heijman, L. Rietveld, Anionic exchange for NOM removal and the effects on micropollutant adsorption competition on activated carbon, Sep. Purif. Technol. 129 (2014) 25–31.